Available online at www.sciencedirect.com
ScienceDirect
Scripta Materialia 57 (2007) 189–192
Scripta MATERIALIA
www.elsevier.com/locate/scriptamat

A high-strength bulk nanocrystalline Al–Fe alloy processed by mechanical alloying and spark plasma sintering

T.T. Sasaki,[a,*] T. Mukai[b] and K. Hono[a,b]

[a] *Graduate School of Pure and Applied Sciences, University of Tsukuba, Ibaraki 305-0047, Japan*
[b] *National Institute for Materials Science, Tsukuba 305-0047, Japan*

Received 31 March 2007; revised 10 April 2007; accepted 12 April 2007
Available online 15 May 2007

A bulk nanocrystalline Al–5 at.% Fe alloy was synthesized by mechanical alloying and spark plasma sintering. The alloy exhibited a very high compressive yield strength of 1 GPa with a plastic strain of 0.3. The alloy consists of coarse α-Al grains that form from powder boundaries and nanocrystalline regions composed of α-Al and Al_6Fe phases. The combination of the coarse and nanoscale grains are considered to be the reason for the large plastic strain in such a high-strength material.

Keywords: Mechanical alloying; Plasma spark sintering; Aluminum alloy; Nanocrystalline alloy

There has been increasing interest in the development of high-strength light alloys in recent years because of the strong demand for weight reductions in automobiles and aircraft. The upper limit of the strength that can be achieved by precipitation hardening of wrought aluminum alloys is in the range 550–600 MPa, so a different approach is required to develop aluminum alloys with much higher strength. Grain refinement is one of the most effective way to strengthen metallic materials, and many investigations have been carried out to achieve ultrahigh-strength from ultrafine-grained microstructures processed by equal channel angular pressing [1], rapid solidification [2], powder metallurgy [3], mechanical milling/alloying, subsequent consolidation processes [4] and vapor quenching [5,6].

Al–TM (TM: transition metals) alloys are expected to show superior elevated temperature mechanical property because of the microstructure stability originating from the low diffusivity of TM in Al. Although the Al–Fe system has been studied for a long time, the limited solubility of Fe in Al of less than 0.03 at.% hinders a sufficient age hardening response [7,8]. The effort to extend the solubility of Fe in an α-Al matrix was made by non-equilibrium processes such as rapid solidification, mechanical alloying or electron beam deposition [5,6,9–13]. These processing routes enable not only the solubility extension of Fe in Al but also the microstructure refinement down to a few tens nanometers. Sasaki et al. reported very high-strength (up to 900 MPa) of a nanocrystalline Al–Fe alloy fabricated by the electron beam deposition technique [5]. The detailed observation of the microstructure by Mukai et al. revealed that the local lattice strain near Fe atoms in the aluminum lattice imparts significant strength to the alloy in conjunction with the nanocrystalline sub-grains and the absence of any second phase [6]. Since these alloys have the form of thin plates with less than 1.5 mm thickness, we attempted to synthesize bulk nanocrystalline Al–Fe alloys by a combination of mechanical alloying and spark plasma sintering (SPS). The SPS involves rapid heating of powder by electric current with the simultaneous application of external pressure. Numerous experimental and theoretical investigations into the process suggest the ability of SPS to produce highly dense compacts which suppress grain coarsening [14–20].

Pure Al (99.9% purity and 53–106 μm in diameter) and Fe (99.9% purity and 53–106 μm in diameter) powders were used as starting materials for the mechanical alloying of Al–5 at.% Fe powder. Ball milling was carried out at room temperature in an argon atmosphere using a Fretsch Pulver-isette P-6 planetary ball mill using stainless steel balls. For the run, 10 g of powder mixture, 100 g of steel balls and 4 wt.% of ethanol were sealed in a stainless steel vial. Mechanically milled powders were consolidated using a SPS machine, Sumitomo Coal Mining Model 1050. A 1.5 g quantity of powder was placed into a 10-mm-diameter tungsten carbide

* Corresponding author. E-mail: sasaki.taisuke@nims.go.jp

1359-6462/$ - see front matter
doi:10.1016/j.scriptamat.2007.04.010

die and sintered under a vacuum of around 4.0×10^{-3} Pa for 5 min at a sintering temperature of 753 K. Tungsten carbide dies were used so that higher loads could be applied for sintering. Vickers hardness measurements were carried out for all the sintered samples under an applied load of 500 g. X-ray diffraction (XRD) analyses were carried out with a RIGAKU RINT-2500 X-ray diffractometer using Cu Kα radiation. The mechanical properties of the sintered samples were evaluated by compression test using cuboidal specimens of $2 \times 2 \times 4$ mm^3 at a strain rate of 1.0×10^{-3} s^{-1}. The microstructure characterizations were carried out using a JEOL JSM-5400 scanning electron microscope (SEM) operating at 15 kV and an FEI Tecnai G^{2}F30 transmission electron microscope (TEM) operating at 300 kV. TEM specimens were prepared by twin-jet electropolishing at a voltage of 20 V and a temperature of 223 K. The electrolyte was a solution of methanol and nitric acid in a ratio of 2:1. Energy-filtered images were recorded on a charge-coupled device camera in a Gatan imaging filter (GIF) Tridium installed on the Tecnai G^{2}F30 TEM. Energy-filtered images were formed by the jump ratio method using the Fe L edge (708 eV) and the O K edge (532 eV) with a 30 and 20 eV window, respectively. An exposure time of 30–40 s was used to acquire each energy-filtered image.

Figure 1 shows a true stress–strain curve of the sintered sample in compression. The stress–strain curve shows a ''work softening''-like feature; the stress value decreases with plastic strain after yielding. The alloy shows very high 0.2% proof stress of 992 MPa with a large plastic strain of 0.3 and a maximum strength of up to 1045 MPa. This value is much higher than that for high-strength wrought aluminum alloys such as Al–Zn–Mg alloy and nanocrystalline Al–Mg alloy, and is comparable with some of amorphous-based aluminum alloys [1–4].

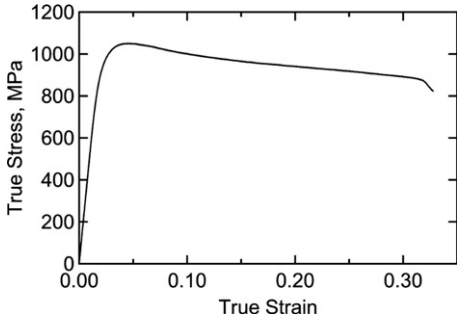

Figure 1. Compressive nominal stress–strain behavior of spark plasma sintered Al–5 at.% Fe alloy.

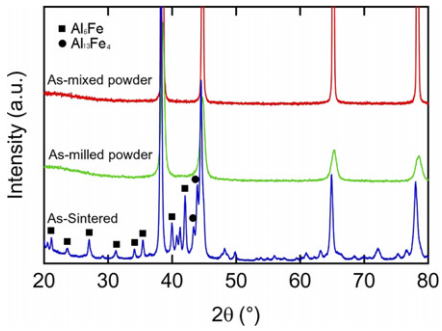

Figure 2. XRD patterns of as-mixed powder, as-milled powder and as-sintered alloy.

Figure 2 shows XRD profiles of the as-mixed powder, as-milled powder and as-sintered alloy. Table 1 summarizes the 2θ values of Al(1 1 1) and Al(3 1 1) diffraction peaks, which do not overlap with any iron peaks, the full-width half maxima (FWHM) of the corresponding peaks, the calculated lattice parameter and the grain size estimated from Hall's method. The Al peaks shift to higher angles, indicating a dissolution of Fe in α-Al by mechanical milling. Mechanical milling also caused peak broadening as a result of the refinement of the crystal grain size and the straining during milling. The estimated grain size of the as-milled powder is 24 nm. After sintering, intermetallic compounds such as Al_6Fe and $Al_{13}Fe_4$ were found. The crystalline Al_6Fe is a metastable phase with an orthorhombic structure (space group *Cmc*21) [21,22]. The α-Al diffraction peaks are sharpened compared with those of the as-milled powder, which is attributed to the grain growth during sintering. The peak shift to a lower angle is due to the depletion of Fe from the α-Al matrix mainly due to the precipitation of the intermetallic compounds, such as Al_6Fe and $Al_{13}Fe_4$.

The density of the sintered sample was 2.91 g cm^{-3}, which is closer to that of Al–5.5 at.% Fe alloy (2.91 g cm^{-3}) rather than that of Al–5 at.% Fe alloy (2.89 g cm^{-3}). This is attributed to the contamination of Fe from the stainless steel vial and balls during the mechanical milling process. The porosity-free feature is confirmed in the secondary electron SEM image shown in Figure 3. Since no porosity is observed in the micrograph, the alloy is thought to have nearly full density. The microstructure consists of three different contrasts: black contrast, tiny particles with white contrast and gray contrast from the matrix. The black contrast was the α-Al phase since only Al was detected by an energy-dispersive spectroscopy (EDS) analysis. The tiny particles are less than 1 μm in diameter. The composition was estimated to be Al–23 at.% Fe by EDS, which is very close to that of the $Al_{13}Fe_4$ phase. Since the XRD

Table 1. Summary of the XRD analysis

	2θ (°)		FWHM		Lattice parameter, a_0 (Å)	Grain size, d (nm)
	Al(1 1 1)	Al(3 1 1)	Al(1 1 1)	Al(3 1 1)		
As-mixed	38.438	78.242	0.141	0.183	2.337	N/A
As-milled	38.572	78.417	0.381	0.593	2.332	24
Sintered	38.231	77.985	0.282	0.401	2.352	N/A